



Local projection stabilization with discontinuous Galerkin method in time applied to convection dominated problems in time-dependent domains

Shweta Srivastava^{1,2} · Sashikumaar Ganesan²

Received: 31 July 2018 / Accepted: 11 November 2019
© Springer Nature B.V. 2019

Abstract

This paper presents the numerical analysis of a stabilized finite element scheme with discontinuous Galerkin (dG) discretization in time for the solution of a transient convection–diffusion–reaction equation in time-dependent domains. In particular, the local projection stabilization and the higher order dG time stepping scheme are used for convection dominated problems. Further, an arbitrary Lagrangian–Eulerian formulation is used to handle the time-dependent domain. The stability and error estimates are given for the proposed numerical scheme. The validation of the proposed local projection stabilization scheme with higher order dG time discretization is demonstrated with appropriate numerical examples.

Keywords Convection–diffusion–reaction equation · Local projection stabilization · Discontinuous Galerkin method in time · Arbitrary Lagrangian Eulerian formulations

Mathematics Subject Classification 65M12 · 65M60 · 35Q35

1 Introduction

The aim of this paper is to analyze the local projection stabilization scheme with discontinuous Galerkin in time for the approximation of singularly perturbed scalar partial differential equations (SPDEs) in time-dependent domains. In this work, the governing equation is designed within the framework of a conservative arbitrary Lagrangian–

✉ Shweta Srivastava
shweta@imca.edu.pe

Sashikumaar Ganesan
sashi@iisc.ac.in

¹ Instituto de Matematica Y Ciencias Afines (IMCA), Universidad Nacional de Ingenieria, Lima, Peru

² Department of Computational and Data Sciences, Indian Institute of Science, Bangalore 560012, India

Eulerian (ALE) formulation. In ALE approach, the boundary moves with a given velocity \mathbf{w} , whereas the inner domain deforms arbitrarily. This is achieved by an ALE map \mathcal{A}_t that maps a reference (initial/previous time step) domain to a current computational domain.

It is well-known that the standard Galerkin solution for convection dominated problems is numerically not appropriate as the discrete solution is polluted with spurious oscillations. Stability and accuracy of the standard Galerkin solution can be enhanced by various stabilization approaches. The idea of streamline upwind Petrov–Galerkin (SUPG) stabilization is first proposed in [11]. Other popular stabilization methods such as Galerkin least-squares [24], edge stabilization [15], continuous interior penalty (CIP) [13,14], subgrid scale stabilization (SGS) [23], orthogonal subscales method (OSS) [2,16,17] have also been proposed in the literature for SPDEs in stationary domains, see [28] for an overview. The main drawback of SUPG stabilization is that various terms including higher order (second) derivative need to be added in the weak form to keep the consistency of the method [12,25,31]. It becomes more complicated in the case of time-dependent equations since the time derivative also need to be included in the weak form to maintain the consistency. An inconsistent SUPG stabilization method for scalar problems in time-dependent domains has been studied in [20,29].

Local projection stabilization (LPS) preserves the stability of the solution and it does not require other terms to be added in stabilization and can easily be implemented [3,27]. This method has originally been proposed for Stokes problem [3], extended to convection dominated scalar problem [4], and to various incompressible flow problems [10]. Application of LPS to convection-diffusion problems with overlapping spaces has been given in [26]. Since LPS is a symmetric stabilization, it can also be used for control problems [5,9].

LPS has originally been given as a two-level method in which projection space D_h lies on a coarser grid, but this approach increases the discretization stencil. Here we concentrate on one-level approach, in which the approximation space V_h and projection space D_h are defined on the same mesh, with enrichment of the approximation space V_h . We first discretize the equation in space with local projection finite element method. The stabilization term in the local projection method is based on a projection $\pi_h : V_h \rightarrow D_h$ of finite element approximation space V_h into a discontinuous space D_h . In LPS, a term which gives L^2 -control over fluctuation κ_h of the gradient of the solution is added. Here, the local projection is incorporated by enriching the approximation space, see [28]. This is known as the one-level LPS, since the approximation and projection spaces lie on the same mesh.

In the previous work [20], it has been shown that SUPG stabilization scheme with implicit Euler and Crank–Nicolson time discretizations behave differently. The first order implicit Euler is unconditionally stable whereas the second order Crank–Nicolson becomes conditionally stable with a restriction on time step Δt . Moreover, it has been observed in the previous studies [6,18,19,29] that both the conservative and non-conservative formulations behave differently. This raises a point to consider higher order discretizations in time. In this work, the higher order discontinuous Galerkin (dG) method is used for the temporal discretization. DG in time on fixed domains can be found in [30]. DG in time for scalar PDEs in time-dependent domains without space

discretization is analyzed in [7,8]. In [1], the local projection scheme with dG in time is given for fixed domain problems.

The paper is organized as follows. In Sect. 2, the transient convection–diffusion equation in a time-dependent domain and its ALE formulations are given. The spatial discretization with local projection finite element method is presented in Sect. 3. Further, the error estimate of the semi-discrete problem (continuous in time) is also derived in this section. Section 4 is devoted to the estimates of the fully discrete problem obtained with discontinuous Galerkin time discretizations. Finally, the numerical studies and a summary are presented in Sects. 5 and 6, respectively.

2 Model problem in time-dependent domain

2.1 Convection–diffusion–reaction equation

Let Ω_t be a time-dependent bounded domain in \mathbb{R}^d , $d = 2, 3$ with Lipschitz boundary $\partial\Omega_t$ for each $t \in [0, T]$, where T is a given end time. Consider a transient convection–diffusion–reaction equation : find $u(x, t) : \Omega \times (0, T] \rightarrow \mathbb{R}$ such that

$$\begin{aligned} \frac{\partial u}{\partial t} - \epsilon \Delta u + \mathbf{b} \cdot \nabla u + cu &= f && \text{in } \Omega_t \times (0, T], \\ u &= 0 && \text{on } \partial\Omega_t \times [0, T], \\ u(x, 0) &= u_0(x) && \text{in } \Omega_0. \end{aligned} \tag{1}$$

Here $u(x, t)$ is an unknown scalar function, $u_0(x)$ is a given initial data, ϵ is a diffusivity constant, $\mathbf{b}(x, t)$ is a convective flow velocity, $c(x, t)$ is a reaction function, $f(x)$ is a given source term with $f \in L^2(\Omega_t)$. Further, assume that there exists a constant μ such that

$$\left(c - \frac{1}{2} \nabla \cdot \mathbf{b} \right) (x, t) \geq \mu > 0, \quad \forall x \in \Omega_t, t \in (0, T). \tag{2}$$

2.2 ALE formulation

Let $\hat{\Omega}$ be a reference domain. The reference domain $\hat{\Omega}$ can simply be the initial domain Ω_0 or the previous time-step domain, when the deformation of the domain is large. Let \mathcal{A}_t be a family of bijective ALE mappings, which at each time $t \in (0, T]$, maps a point Y of a reference domain $\hat{\Omega}$ to a point on the current domain Ω_t , given by

$$\mathcal{A}_t : \hat{\Omega} \rightarrow \Omega_t, \quad \mathcal{A}_t(Y) = x(Y, t), \quad t \in (0, T).$$

Moreover, for any time $t_1, t_2 \in [0, T]$, the ALE mapping between two time instances will be given by,

$$\mathcal{A}_{t_1, t_2} : \Omega_{t_1} \rightarrow \Omega_{t_2} \quad \mathcal{A}_{t_1, t_2} = \mathcal{A}_{t_2} \circ \mathcal{A}_{t_1}^{-1}.$$

The domain velocity \mathbf{w} is defined as

$$\mathbf{w}(x, t) = \left. \frac{\partial x}{\partial t} \right|_Y (\mathcal{A}_t^{-1}(x), t).$$

Further, we assume that Ω_t is bounded with Lipschitz continuous boundary for each $t \in [0, T]$. For a function $u \in C^0(\Omega_t)$ on the Eulerian frame, we define the corresponding function $\hat{u} \in C^0(\hat{\Omega})$ on the ALE frame as

$$\hat{u} : \hat{\Omega} \times (0, T) \rightarrow \mathbb{R}, \quad \hat{u} := u \circ \mathcal{A}_t, \quad \text{with} \quad \hat{u}(Y, t) = u(\mathcal{A}_t(Y), t).$$

The temporal derivative on the ALE frame is defined as

$$\left. \frac{\partial u}{\partial t} \right|_Y : (x, t) \rightarrow \mathbb{R}, \quad \left. \frac{\partial u}{\partial t} \right|_Y (x, t) = \frac{\partial \hat{u}}{\partial t}(Y, t), \quad Y = \mathcal{A}_t^{-1}(x).$$

Applying the chain rule to the time derivative of $u \circ \mathcal{A}_t$ on the ALE frame to get

$$\left. \frac{\partial u}{\partial t} \right|_Y = \frac{\partial u}{\partial t}(x, t) + \left. \frac{\partial x}{\partial t} \right|_Y \cdot \nabla_x u = \frac{\partial u}{\partial t} + \frac{\partial \mathcal{A}_t(Y)}{\partial t} \cdot \nabla_x u = \frac{\partial u}{\partial t} + \mathbf{w} \cdot \nabla_x u.$$

By using the relation in the model problem (1), we get

$$\left. \frac{\partial u}{\partial t} \right|_Y - \epsilon \Delta u + (\mathbf{b} - \mathbf{w}) \cdot \nabla u + cu = f. \quad (3)$$

This equation is the non-conservative ALE counterpart of the model equation (1). Alternatively, we can use the Reynolds transport theorem to derive the conservative ALE-form of the equation.

$$\begin{aligned} \frac{d}{dt} \int_{\Omega_t} u \, dx &= \int_{\hat{\Omega}} \frac{\partial(u J_{A_t})}{\partial t} dY = \int_{\hat{\Omega}} \left[J_{A_t} \left. \frac{\partial u}{\partial t} \right|_Y + u \frac{\partial J_{A_t}}{\partial t} \right] dY \\ &= \int_{\hat{\Omega}} \left[\left. \frac{\partial u}{\partial t} \right|_Y + u \nabla \cdot \mathbf{w} \right] J_{A_t} dY \\ &= \int_{\Omega_t} \left(\frac{\partial u}{\partial t} + \mathbf{w} \cdot \nabla u + u \nabla \cdot \mathbf{w} \right) dx, \end{aligned} \quad (4)$$

here we have used the Euler expansion formula given by

$$\left. \frac{\partial \mathbf{J}_{A_t}}{\partial t} \right|_Y = \mathbf{J}_{A_t} \nabla \cdot \mathbf{w}. \quad (5)$$

Here, $J_{A_t} = \det(\mathbf{J}_{A_t})$ and the Jacobian matrix of the ALE mapping, \mathbf{J}_{A_t} is given by

$$\mathbf{J}_{A_t} = \frac{\partial x_i}{\partial Y_j}, \quad 1 \leq i, j \leq d.$$

Now using the Reynolds transport theorem, the conservative ALE form of Eq. (1) can be written as

$$\frac{\partial(uJ_{A_t})}{\partial t} \Big|_Y + J_{A_t} [-\epsilon \Delta u + (\mathbf{b} - \mathbf{w}) \cdot \nabla u + (c - \nabla \cdot \mathbf{w})u] = J_{A_t} f. \tag{6}$$

2.3 Variational form

In this section, the finite element variational form of the ALE Eqs. (3) and (6) are derived. Let

$$V = \left\{ v \in H_0^1(\Omega_t), \quad v : \Omega_t \times (0, T] \rightarrow \mathbb{R}, \quad v = \hat{v} \circ \mathcal{A}_t^{-1}, \quad \hat{v} \in H_0^1(\hat{\Omega}) \right\},$$

be the solution space for Eqs. (3) and (6). The L^2 -inner product, the L^2 -norm and the H^1 semi-norm, $(\cdot, \cdot)_t$, $\|\cdot\|_t$ and $|\cdot|_{1,t}$, respectively, over Ω_t are defined as

$$(u, v)_t := \int_{\Omega_t} uv \, dx, \quad \|v\|_t^2 := (v, v)_t, \quad |v|_{1,t}^2 := (\nabla v, \nabla v)_t, \quad \forall u, v \in V.$$

Further, let X be a Banach space equipped with the norm $\|\cdot\|_X$, then we define

$$\begin{aligned} C(0, T; X) &= \{v : [0, T] \rightarrow X, \quad v \text{ is continuous}\}, \\ L^2(0, T; X) &= \left\{ v : (0, T) \rightarrow X, \quad \int_0^T \|v(t)\|_X^2 dt < \infty \right\}, \\ H^m(0, T; X) &= \left\{ v \in L^2(0, T; X) : \frac{\partial^i v}{\partial t^i} \in L^2(0, T; X), \quad 1 \leq i \leq m \right\}. \end{aligned}$$

Using the short notation for space as $Y(X) := Y(0, T; X)$, we write the norms in the above space

$$\begin{aligned} \|v\|_{C(X)} &= \sup_{t \in [0, T]} \|v(t)\|_X, & \|v\|_{L^2(X)}^2 &= \int_0^T \|v(t)\|_X^2 dt, \\ |v|_{H^m(X)}^2 &= \int_0^T \left\| \frac{\partial^m v}{\partial t^m} \right\|_X^2 dt, & \|v\|_{H^m(X)}^2 &= \int_0^T \sum_{i=0}^m \left\| \frac{\partial^i v}{\partial t^i} \right\|_X^2 dt. \end{aligned}$$

Now multiplying Eq. (3) with a test function $v \in V$ and applying integration by parts to the higher order derivative term, the variational form of Eq. (3) reads:

For given $\hat{\Omega}$, \mathbf{b} , \mathbf{w} , c , u_0 and $f \in L^2(\Omega_t)$, find $u \in L^2(0, T; V)$ such that for all $v \in L^2(0, T; V)$ and $t_1, t_2 \in (0, T]$ with $t_1 < t_2$,

$$\begin{aligned}
& \int_{t_1}^{t_2} \left[\left(\frac{\partial u}{\partial t} \Big|_Y, v \right)_t + (\epsilon \nabla u, \nabla v)_t + ((\mathbf{b} - \mathbf{w}) \cdot \nabla u, v)_t + (cu, v)_t \right] dt \\
&= \int_{t_1}^{t_2} (f, v)_t dt, \\
&(u, v) = (u_0, v)_0.
\end{aligned} \tag{7}$$

Similarly, the conservative ALE weak form of Eq. (7) can be written as: For given $\hat{\Omega}$, \mathbf{b} , \mathbf{w} , c , u_0 and $f \in L^2(\Omega_t)$, find $u \in L^2(0, T; V)$ such that for all $v \in L^2(0, T; V)$

$$\begin{aligned}
& (u, v)_{t_2} + \int_{t_1}^{t_2} \left[(\epsilon \nabla u, \nabla v)_t + ((\mathbf{b} - \mathbf{w}) \cdot \nabla u, v)_t + ((c - \nabla \cdot \mathbf{w})u, v)_t \right. \\
& \quad \left. - \left(u, \frac{\partial v}{\partial t} \Big|_Y \right)_t \right] dt \\
&= (u, v)_{t_1} + \int_{t_1}^{t_2} (f, v)_t dt, \\
&(u, v) = (u_0, v)_0.
\end{aligned} \tag{8}$$

The main difference between (1) and (7), (8) is the additional domain velocity \mathbf{w} in the ALE form that accounts for the deformation of the domain. In this work, we consider the conservative-ALE form of Eq. (8).

3 Stabilization by local projection finite element

Let $\mathcal{T}_{h,0}$ denote a shape regular triangulation of the initial domain Ω_0 into simplices. Further, $\mathcal{T}_{h,t}$, $t \in (0, T]$ be the triangulation of Ω_t into simplices obtained by ALE mapping from $\mathcal{T}_{h,0}$. Further, we denote the diameter of the cell $K \in \mathcal{T}_{h,t}$ by $h_{K,t}$ and the global mesh size by $h_t := \max\{h_{K,t} : K \in \mathcal{T}_{h,t}\}$. We now define the discrete ALE mapping $\mathcal{A}_{h,t}(Y)$ and the mesh velocity \mathbf{w}_h in space. We use the Lagrangian finite element space

$$\mathcal{L}^k(\hat{\Omega}) = \left\{ \psi \in H^k(\hat{\Omega}) : \psi|_K \in P_k(\hat{K}) \text{ for all } \hat{K} \in \hat{\Omega}_h \right\}.$$

Using the linear space, we define the semi-discrete ALE mapping in space for each $t \in [0, T]$ by

$$\mathcal{A}_{h,t} : \hat{\Omega}_h \rightarrow \Omega_{h,t}. \tag{9}$$

Further, the semi-discrete (continuous in time) mesh velocity $\mathbf{w}_h(t, Y) \in \mathcal{L}^1(\hat{\Omega})^d$ in the ALE frame for each $t \in [0, T]$ is defined by

$$\hat{\mathbf{w}}_h(t, Y) = \sum_{i=1}^{\mathcal{M}} \mathbf{w}_i(t) \psi_i(Y); \quad \mathbf{w}_i(t) \in \mathbb{R}^d.$$

Here, $\mathbf{w}_i(t)$ denotes the mesh velocity of the i^{th} node of simplices at time t , and $\psi_i(Y)$, $i = 1, 2, \dots, \mathcal{M}$, are the basis functions of $\mathcal{L}^1(\hat{\Omega}_h)^d$. We then define the semi-discrete mesh velocity in the Eulerian frame as

$$\mathbf{w}_h(x, t) = \hat{\mathbf{w}}_h \circ \mathcal{A}_{h,t}^{-1}(x).$$

To write the continuous equation in triangulated domain, we will first make the hypothesis that the domain Ω_t can exactly be represented by the discrete ALE map, that is, $\Omega_{h,t} = \Omega_t, \forall t \in I$. Thus, we can make use of discrete ALE mapping and write the continuous equation (8) in the weak ALE form: find $u \in L^2(0, T; V)$ such that

$$(u, v)_{h,t_2} + \int_{t_1}^{t_2} \left[(\epsilon \nabla u, \nabla v)_{h,t} + ((\mathbf{b} - \mathbf{w}_h) \cdot \nabla u, v)_{h,t} + ((c - \nabla \cdot \mathbf{w}_h)u, v)_{h,t} - \left(u, \frac{\partial v}{\partial t} \Big|_Y \right)_{h,t} \right] dt = (u, v)_{h,t_1} + \int_{t_1}^{t_2} (f, v)_{h,t} dt, \quad \forall v \in L^2(0, T; V). \tag{10}$$

Suppose $V_h \subset V$ is a conforming finite dimensional subspace of V and D_h be the projection space of discontinuous piecewise polynomials. Let $\pi_K : L^2(K) \rightarrow D_h(K)$ be a local projection into the space $D_h(K)$. Define the global projection $\pi_h : L^2(\Omega_t) \rightarrow D_h$ by $(\pi_h v)|_K := \pi_K(v|_K)$. Further, associate a fluctuation operator $\kappa_h : L^2(\Omega_t) \rightarrow L^2(\Omega_t)$ which is defined by $\kappa_h := I_d - \pi_h$, where $I_d : L^2(\Omega_t) \rightarrow L^2(\Omega_t)$ is the identity map. Then, the local projection stabilization is based on the following assumptions (see [28]):

Assumption 1 *There exist an interpolation operator $i_h : H^2(\Omega) \rightarrow V_h$ such that for all $K \in \mathcal{T}_{h,t}$*

$$\|v - i_h v\|_K + h_K |v - i_h v|_{1,K} \leq Ch_K^l \|v\|_{l,K}, \quad \forall v \in H^l(K), \text{ with } 2 \leq l \leq r + 1.$$

Assumption 2 *The orthogonality property is given as*

$$(v - i_h v, q_h) = 0 \quad \forall q_h \in D_h, \quad \forall v \in H^2(\Omega).$$

Assumption 3 *The fluctuation operator κ_h satisfies the following approximation property,*

$$\|\kappa_h v\|_K \leq Ch_K^l \|v\|_{l,K} \quad \forall v \in H^l(K), \quad 0 \leq l \leq r.$$

We use mapped finite element spaces that satisfy the above assumptions, where the enriched approximation spaces on the reference cell \hat{K} are given by

$$\begin{aligned} P_r^{bubble}(\hat{K}) &:= P_r(\hat{K}) \oplus (\hat{b}_\Delta \cdot P_{r-1}(\hat{K})) \\ Q_r^{bubble}(\hat{K}) &:= Q_r(\hat{K}) \oplus \text{span} \left\{ \hat{b}_\square \cdot \hat{x}_i^{r-1}, \quad i = 1, 2 \right\}, \end{aligned}$$

Here, \hat{b}_Δ and \hat{b}_\square are the cubic bubble and the bi-quadratic bubble functions on the reference triangle and quadrilateral, respectively see [21]. On triangular cells, we use $(V_h, D_h) = (P_r^{bubble}, P_{r-1}^{disc})$, whereas on quadrilateral cells, we use $(V_h, D_h) = (Q_r^{bubble}, P_{r-1}^{disc})$. The stabilization term corresponding to LPS is given by,

$$S_h(u_h, v_h) = \sum_{K \in \mathcal{T}_{h,t}} \tau_K (\kappa_h \nabla u_h, \kappa_h \nabla v_h)_K. \tag{11}$$

Here, τ_K is an user chosen stabilization parameter, whose value depends on the mesh size and the convective velocity [27].

Now, using the local projection stabilization to the conservative ALE form (10), the semi-discrete problem reads: find $u_h \in L^2(0, T : V_h)$ such that for all $v_h \in L^2(0, T : V_h)$, $t_1, t_2 \in (0, T]$ with $t_1 < t_2$,

$$\begin{aligned} (u_h, v_h)_{h,t_2} + \int_{t_1}^{t_2} \left[a_{LPS}(u_h, v_h)_{h,t} - (\nabla \cdot (\mathbf{w}_h u_h), v_h)_{h,t} - \left(u_h, \frac{\partial v_h}{\partial t} \Big|_Y \right)_{h,t} \right] dt \\ = (u_h, v_h)_{h,t_1} + \int_{t_1}^{t_2} (f(t), v_h)_{h,t} dt, \end{aligned} \tag{12}$$

where,

$$\begin{aligned} a_{LPS}(u_h, v_h)_{h,t} = \epsilon (\nabla u_h, \nabla v_h)_{h,t} + (\mathbf{b} \cdot \nabla u_h, v_h)_{h,t} + (cu_h, v_h)_{h,t} \\ + \sum_{K \in \mathcal{T}_{h,t}} \tau_K (\kappa_h \nabla u_h, \kappa_h \nabla v_h)_K. \end{aligned}$$

The subscript h in the inner product $(\cdot, \cdot)_{h,t}$ denotes that the integral is over the triangulated domain. Nevertheless, we will not explicitly mention hereafter and skip the subscript h .

Lemma 1 *Coercivity of $a_{LPS}(\cdot, \cdot)$: Let the discrete form of the assumptions (2) be satisfied. Further, assume that the stabilization parameter satisfies $\tau_K \sim O(h_{K,t})$. Then, the bilinear form satisfies*

$$a_{LPS}(u_h, u_h)_t \geq |||u_h(t)|||_t^2, \tag{13}$$

where the mesh-dependent norm is defined as

$$|||u_h|||_t^2 = \left(\epsilon |u_h|_{1,t}^2 + \sum_{K \in \mathcal{T}_{h,t}} \tau_K \|\kappa_h \nabla u_h\|_K^2 + \mu |u_h|_t^2 \right).$$

Proof Substitute $v_h = u_h$ in the definition of bilinear form $a_{LPS}(u_h, v_h)_{h,t}$ given above, and use the discrete form of assumption (2), the coercivity (13) can be derived. \square

Remark 1 Here we have considered the full gradient in the stabilization. Nevertheless, the stabilization can also be added in the streamline direction $(\mathbf{b} - \mathbf{w}_h)$. The fluctuation operator of the convective derivative in stabilization needs further investigation in analysis and as well as in implementation. Though the full gradient is considered, it is shown with the numerical results that the LPS scheme works well for the convection dominated boundary/interior layer problems.

We next define the Ritz projection $R_h : V \rightarrow V_h$ in order to analyze the semi-discrete error for problems defined in time-dependent domains. Let $R_h v \in V_h$, then the Ritz projection will be given by,

$$a_{LPS}(R_h u, v_h) - (\nabla \cdot (\mathbf{w}_h R_h u), v_h) = a(u, v_h) - (\nabla \cdot (\mathbf{w}_h u), v_h). \tag{14}$$

Here the bilinear form $a(u, v)$ is given as

$$a(u, v)_t = \epsilon (\nabla u, \nabla v)_t + (\mathbf{b} \cdot \nabla u, v)_t + (cu, v)_t. \tag{15}$$

Lemma 2 *Let the Assumptions 1 and 2 hold true, $\tau_K \sim O(h_{K,t})$ and the data of the problem be sufficiently smooth. Then, there exists a positive constant c , such that*

$$|||R_h u||| \leq c |||u|||_1, \tag{16}$$

and

$$|||u - R_h u||| \leq c(\epsilon^{1/2} + h^{1/2})h^r |||u|||_{r+1}. \tag{17}$$

Here, $|| \cdot ||_{r+1}$ denote the norm in $H^{r+1}(\Omega_t)$.

Proof Using the definition of $||| \cdot |||$ -norm, we get

$$\begin{aligned} |||R_h u|||^2 &= a_{LPS}(R_h u, R_h u) = a(u, R_h u) + (\nabla \cdot (\mathbf{w}_h R_h u), R_h u) - (\nabla \cdot (\mathbf{w}_h u), R_h u) \\ &= a(u, R_h u) + (\nabla \cdot (\mathbf{w}_h (R_h u - u)), R_h u) \\ &\leq |||u|||_1 |||R_h u||| + (||\nabla \cdot \mathbf{w}_h||_\infty ||R_h u - u|| + ||\mathbf{w}_h||_\infty ||\nabla \cdot (R_h u - u)||) |||R_h u|| \\ &\leq |||u|||_1 |||R_h u||| + (||\nabla \cdot \mathbf{w}_h||_\infty ||R_h u - u|| + ||\mathbf{w}_h||_\infty ||R_h u - u||) |||R_h u|| \\ &\leq |||u|||_1 |||R_h u||| + (||\nabla \cdot \mathbf{w}_h||_\infty + ||\mathbf{w}_h||_\infty) ||R_h u - u|| |||R_h u|| \\ &\leq c |||u|||_1 |||R_h u|||. \end{aligned}$$

Here, we have used the fact that the mesh velocity is bounded. The Ritz projection error, $||R_h u - u|| \leq |||R_h u - u||| \leq c(\epsilon^{1/2} + h^{1/2})h^r |||u|||_{r+1}$, is bounded from the second part of the lemma [28] and hence the proof of the first part of the lemma can be followed. For the second part, (see [28, p. 343]). \square

Theorem 1 (Error estimate for the ALE-LPS form of semi-discrete scheme) *Let the Assumptions 1, 2 and the discrete form of Eq. (2) be satisfied. Let $u(t)$ and $u_h(t)$ be the solution of continuous problem (10) and semi-discrete problem (12). Further, assume*

that the stabilization parameter satisfies $\tau_K \sim O(h_{K,t})$, then the semi-discrete error satisfies

$$\|u_h(t) - u(t)\| \leq \|u_{h,0} - u_0\| + c(\epsilon^{1/2} + h^{1/2})h^r \left(\|u_0\|_{r+1} + \int_0^t (\|u(t)\|_{r+1} + \|u'(t)\|_{r+1}) dt \right).$$

Proof Substitute $v = v_h$ and subtract the continuous equation (10) with semi-discrete equation (12). Further, split the errors into two parts with Ritz projection term as,

$$u_h(t) - u(t) = u_h(t) - R_h u(t) + R_h u(t) - u(t) = \eta(t) + \xi(t).$$

We can write the error equation as,

$$\begin{aligned} (\eta(t), v_h)_{t_2} + \int_{t_1}^{t_2} \left[a_{LPS}(\eta(t), v_h)_t - (\nabla \cdot (\mathbf{w}_h \eta(t)), v_h)_t - \left(\eta(t), \frac{\partial v_h}{\partial t} \Big|_Y \right)_t \right] dt \\ - (\eta(t), v_h)_{t_1} = (\xi(t), v_h)_{t_2} - (\xi(t), v_h)_{t_1} - \int_{t_1}^{t_2} \left(\xi(t), \frac{\partial v_h}{\partial t} \Big|_Y \right)_t dt. \end{aligned} \tag{18}$$

Set $v_h = \eta$ in (18). Applying integration by parts to the third term of left hand side, we get

$$\int_{\Omega_{h,t}} \nabla \cdot (\mathbf{w}_h \eta) \eta \, dx = - \int_{\Omega_{h,t}} \mathbf{w}_h \cdot \nabla \eta \, dx = \frac{1}{2} \int_{\Omega_{h,t}} \eta^2 \nabla \cdot \mathbf{w}_h \, dx.$$

Using the Euler expansion (5), the fourth term on left hand side can be written as

$$\begin{aligned} \int_{\Omega_{h,t}} \eta \frac{\partial \eta}{\partial t} \Big|_Y \, dx &= \int_{\hat{\Omega}} \eta \frac{\partial \eta}{\partial t} J_{A_t} \, dY = \frac{1}{2} \frac{d}{dt} \int_{\hat{\Omega}} (\eta^2 J_{A_t}) \, dY - \frac{1}{2} \int_{\hat{\Omega}} \eta^2 \frac{\partial J_{A_t}}{\partial t} \, dY \\ &= \frac{1}{2} \frac{d}{dt} \int_{\hat{\Omega}} \eta^2 J_{A_t} \, dY - \frac{1}{2} \int_{\hat{\Omega}} \eta^2 \nabla \cdot \mathbf{w}_h J_{A_t} \, dY \\ &= \frac{1}{2} \left(\frac{d}{dt} \|\eta\|_t^2 - \int_{\Omega_{h,t}} \eta^2 \nabla \cdot \mathbf{w}_h \, dx \right). \end{aligned}$$

For the last term of right hand side, using integration by parts in time and Euler expansion formula (5), we obtain,

$$\begin{aligned} \int_{t_1}^{t_2} \left(\xi(t), \frac{\partial \eta}{\partial t} \Big|_Y \right)_t \, dt \\ = (\xi(t), \eta(t))_{t_2} - (\xi(t), \eta(t))_{t_1} - \int_{\hat{\Omega}} \left(\int_{t_1}^{t_2} \frac{\partial}{\partial t} (\xi(t) J_{A_t}) \eta(t) \, dt \right) \, dY \\ = (\xi(t), \eta(t))_{t_2} - (\xi(t), \eta(t))_{t_1} - \int_{\hat{\Omega}} \int_{t_1}^{t_2} \left(\frac{\partial \xi}{\partial t} J_{A_t} + \xi(t) \nabla \cdot \mathbf{w}_h J_{A_t} \right) \eta(t) \, dt \, dY \end{aligned}$$

$$\begin{aligned}
 &= (\xi(t), \eta(t))_{t_2} - (\xi(t), \eta(t))_{t_1} - \int_{t_1}^{t_2} \int_{\Omega_{h,t}} \left(\frac{\partial \xi}{\partial t} + \xi(t) \nabla \cdot \mathbf{w}_h \right) \eta(t) \, dx \, dt \\
 &= (\xi(t), \eta(t))_{t_2} - (\xi(t), \eta(t))_{t_1} - \int_{t_1}^{t_2} \left(\left(\frac{\partial \xi}{\partial t} + \xi(t) \nabla \cdot \mathbf{w}_h \right), \eta(t) \right)_t \, dt. \tag{19}
 \end{aligned}$$

Further, using the coercivity of bilinear form (13) and the above equalities, Eq. (18) becomes

$$\begin{aligned}
 &\frac{1}{2} \|\eta(t)\|_{t_2}^2 - \frac{1}{2} \|\eta(t)\|_{t_1}^2 + \int_{t_1}^{t_2} \|\eta(t)\|^2 \, dt \\
 &\leq (\xi(t), \eta(t))_{t_2} - (\xi(t), \eta(t))_{t_1} - \int_{t_1}^{t_2} \left(\xi(t), \frac{\partial \eta(t)}{\partial t} \Big|_Y \right)_t \, dt \\
 &= \int_{t_1}^{t_2} \left(\left(\frac{\partial \xi}{\partial t} + \xi(t) \nabla \cdot \mathbf{w}_h \right), \eta(t) \right)_t \, dt \\
 &\leq \int_{t_1}^{t_2} \left(\left\| \frac{\partial \xi}{\partial t} \right\|^2 + \|\nabla \cdot \mathbf{w}_h\|_\infty \|\xi(t)\|^2 + \|\eta(t)\|^2 \right) \, dt.
 \end{aligned}$$

Here, we have used the Cauchy–Schwarz and Young’s inequality for the right hand side terms. Now absorbing the last term of RHS in $\|\eta(t)\|^2$ -norm of LHS, we obtain

$$\|\eta(t)\|_{t_2}^2 + 2 \int_{t_1}^{t_2} \|\eta(t)\|^2 \, dt \leq 2 \|\eta(t)\|_{t_1}^2 + 2 \int_{t_1}^{t_2} \left(\left\| \frac{\partial \xi}{\partial t} \right\|^2 + \|\xi(t)\|_t^2 \right) \, dt,$$

using the non-negativity of $\|\eta(t)\|^2$ -norm term in LHS, we get

$$\|\eta(t)\|_{t_2}^2 \leq 2 \|\eta(t)\|_{t_1}^2 + 2 \int_{t_1}^{t_2} \left(\|\xi'(t)\|_t^2 + \|\xi(t)\|_t^2 \right) \, dt,$$

and the semi-discrete error becomes,

$$\begin{aligned}
 \|u_h(t) - u(t)\| &\leq \|\eta(t)\| + \|\xi(t)\| \leq 2 \|\eta(t)\|_0 + 2 \int_0^t (\|\xi(t)\|_t + \|\xi'(t)\|_t) \, dt \\
 &\leq c \left(\|u_{h,0} - R_h u_0\| + \int_0^t (\|\xi(t)\|_t + \|\xi'(t)\|_t) \, dt \right) \\
 &\leq c \left(\|u_{h,0} - u_0\| + \|u_0 - R_h u_0\| + h^r (\epsilon^{1/2} + h^{1/2}) \right. \\
 &\quad \left. \int_0^t (\|u(t)\|_{r+1} + \|u'(t)\|_{r+1}) \, dt \right) \\
 &\leq c \left(\|u_{h,0} - u_0\| + h^r (\epsilon^{1/2} + h^{1/2}) \left\{ \|u_0\|_{r+1} \right. \right. \\
 &\quad \left. \left. + \int_0^t (\|u(t)\|_{r+1} + \|u'(t)\|_{r+1}) \, dt \right\} \right).
 \end{aligned}$$

□

4 Fully discrete form with dG time discretization

In this section, we present the stability and error estimates for the fully discrete scheme. Let $0 = t_0 < t_1 < \dots < t_N = T$ be a partition of the time interval $[0, T]$ into N uniform time intervals with $I_n = (t_n, t_{n+1}]$. Next, denote the time step by $\Delta t = t_{n+1} - t_n$, $0 \leq n \leq N - 1$. Further,

$$Q_T = \left\{ (x, t) \in \mathbb{R}^d \times \mathbb{R} : t \in [0, T], x = \mathcal{A}_t(y), y \in \Omega_0 \right\}, \quad (20)$$

and

$$Q_n = \{(x, t) \in Q_T : t \in I_n\}. \quad (21)$$

For $q \geq 0$, the discrete space $S_{r,q}$ denotes dG in time of order q , so for the problem in time-dependent domains,

$$S_{r,q} := \left\{ v : Q_T \rightarrow \mathbb{R} : v|_{I_n} = \sum_{j=0}^q \phi_j t^j \text{ with } \phi_j \in V_h \text{ and } \left. \frac{\partial \phi_j}{\partial t} \right|_Y = 0, j=0, \dots, q \right\},$$

and

$$S_{r,q}(I_n) := \{v : Q_n \rightarrow \mathbb{R} : v = w|_{Q_n}, w \in S_{r,q}\}, \quad n=0, 1, \dots, N-1, \quad (22)$$

is the space of restrictions of functions in $S_{r,q}$ to Q_n . Note that no continuity of $U_h(t)$ is required at the nodes $t = t_n$. Further, $U_h(t_n^+)$ is the limit of $U_h(t)$ at t_n from above. Now we discretize the ALE mapping in time using linear interpolation. We denote the discrete ALE mapping by $\mathcal{A}_{h,\Delta t}$, and define it for every $\tau \in [t^n, t^{n+1}]$ by

$$\mathcal{A}_{h,\Delta t}(Y) = \frac{\tau - t^n}{\Delta t} \mathcal{A}_{h,t^{n+1}}(Y) + \frac{t^{n+1} - \tau}{\Delta t} \mathcal{A}_{h,t^n}(Y),$$

where $\mathcal{A}_{h,t}(Y)$ is the time continuous ALE mapping defined in (9). Since the discrete ALE mapping is defined linearly in time, we obtain the discrete mesh velocity

$$\hat{\mathbf{w}}_h^{n+1}(Y) = \frac{\mathcal{A}_{h,t^{n+1}}(Y) - \mathcal{A}_{h,t^n}(Y)}{\Delta t}$$

as a piecewise constant function in time. Further, we define the mesh velocity on the Eulerian frame as

$$\mathbf{w}_h^{n+1} = \hat{\mathbf{w}}_h^{n+1} \circ \mathcal{A}_{h,\Delta t}^{-1}(x).$$

Now, the fully discrete conservative ALE equation with LPS in space and dG in time is given as,

$$\begin{aligned}
 & (U_h(t_{n+1}), v_h(t_{n+1}))_{t_{n+1}} - (U_h(t_n), v_h(t_n^+))_{t_n} + \int_{I_n} a_{LPS}(U_h(t), v_h)_t \, dt \\
 & - \int_{I_n} (\nabla \cdot (\mathbf{w}_h U_h), v_h)_t \, dt - \int_{I_n} \left(U_h, \frac{\partial v_h}{\partial t} \Big|_Y \right)_t \, dt \\
 & = \int_{I_n} (f, v_h)_t \, dt, \forall v_h \in S_{r,q}(I_n),
 \end{aligned} \tag{23}$$

where,

$$\begin{aligned}
 a_{LPS}(U_h, v_h)_t &= \epsilon (\nabla U_h, \nabla v_h)_t + (\mathbf{b} \cdot \nabla U_h, v_h)_t + (c U_h, v_h)_t \\
 &+ \sum_{K \in \mathcal{T}_{h,t}} \tau_K (\kappa_h \nabla U_h, \kappa_h \nabla v_h)_K.
 \end{aligned}$$

Note that the integrals of U_h^n on a domain Ω_{t_s} with $t_s \neq t_n$ is written through the ALE mapping

$$\int_{\Omega_{t_s}} U_h(t_n) \, dx = \int_{\Omega_{t_s}} U_h(t_n) \circ \mathcal{A}_{t_n, t_s} \, dx.$$

Remark 2 It can be observed that the terms

$$\int_{\Omega_t} \frac{\partial U_h}{\partial t} \Big|_Y v_h \, dx, \int_{\Omega_t} \mathbf{w}_h \cdot \nabla U_h v_h \, dx, \int_{\Omega_t} \nabla \cdot \mathbf{w}_h U_h v_h \, dx$$

are polynomial of order $(2q + dq' - 1)$ in time, where q' is the order of the polynomial for approximating the ALE map. In numerical test cases, we use the second order discontinuous Galerkin dG(1) in time i.e. $q = 1$ with dimension $d = 2$. Further, we use linear interpolation in time for the discrete ALE mapping, i.e. $q' = 1$. Hence, we need a quadrature in time, which is exact for polynomials of order $2q' + 1 = 3$.

4.1 Stability estimate of fully discrete conservative ALE-LPS form with dG time discretization

In this section, the stability of conservative ALE- LPS with dG discretization in time is considered.

Further, the discrete ALE mapping satisfies,

$$\mathcal{A}_{h,t} \in W_\infty^1(\Omega_0), \text{ and } \mathcal{A}_{h,t}^{-1} \in W_\infty^1(\Omega_t). \tag{24}$$

Thus, the quantity $\|\mathcal{A}_{h,t}\|_{L^\infty(\Omega_0 \times I)}$ is finite and bounded [8,22].

Theorem 2 (Stability estimate for the conservative ALE-LPS form and dG in time) *Let the discrete form of (2) be satisfied. Further, assume that the stabilization parameter satisfies $\tau_K \sim O(h_{K,t})$, then the solution of (23) satisfies*

$$\begin{aligned} & \|U_h(t_N)\|_{t_N}^2 + \int_0^{t_N} \|U_h(t)\|_t^2 dt + \sum_{n=0}^{N-1} \|(U_h(t_n^+) - U_h(t_n))\|_{t_n}^2 \\ & \leq \|U_h(0)\|_{t_0}^2 + \frac{1}{\mu} \int_0^{t_N} \|f(t)\|_t^2 dt. \end{aligned}$$

Proof Take $v_h = U_h$ in equation (23),

$$\begin{aligned} & \|U_h(t_{n+1})\|_{t_{n+1}}^2 - (U_h(t_n), U_h(t_n^+))_{t_n} + \int_{I_n} a_{LPS}(U_h(t), U_h(t))_t dt \\ & - \int_{I_n} (\nabla \cdot (\mathbf{w}_h U_h), U_h)_t dt - \int_{I_n} \left(U_h, \frac{\partial U_h}{\partial t} \Big|_Y \right)_t dt = \int_{I_n} (f, U_h)_t dt, \quad (25) \end{aligned}$$

using the estimates for the left hand side terms,

$$(U_h(t_n), U_h(t_n^+))_{t_n} = \frac{1}{2} \left(\|U_h(t_n)\|_{t_n}^2 + \|U_h(t_n^+)\|_{t_n}^2 - \|U_h(t_n^+) - U_h(t_n)\|_{t_n}^2 \right), \quad (26)$$

$$\int_{I_n} \left(U_h, \frac{\partial U_h}{\partial t} \Big|_Y \right)_t dt = \frac{1}{2} \left(\|U_h(t_{n+1})\|_{t_{n+1}}^2 - \|U_h(t_n^+)\|_{t_n}^2 - \int_{I_n} (\nabla \cdot \mathbf{w}_h, U_h^2)_t \right), \quad (27)$$

$$\left| \int_{I_n} (f, U_h)_t dt \right| \leq \frac{1}{2\mu} \int_{I_n} \|f(t)\|_t^2 dt + \frac{\mu}{2} \int_{I_n} \|U_h(t)\|_t^2 dt. \quad (28)$$

Substitute all these estimates, and using the coercivity of bilinear form $a_{LPS}(U_h(t), U_h(t))$, Eq. (25) becomes,

$$\begin{aligned} & \|U_h(t_{n+1})\|_{t_{n+1}}^2 + \|U_h(t_n^+) - U_h(t_n)\|_{t_n}^2 + \int_{I_n} \|U_h(t)\|_t^2 dt \\ & \leq \|U_h(t_n)\|_{t_n}^2 + \frac{1}{\mu} \int_{I_n} \|f(t)\|_t^2 dt. \end{aligned}$$

summing over the index $n = 0, 1, 2, \dots, N-1$, the stability estimate for fully discrete problem is derived. It can be seen that the higher order dG time discretization is unconditionally stable that means there is no time step (Δt) restriction. \square

Remark 3 Here we considered the conservative ALE form. For $q = 0$, dG(0) corresponds to the implicit Euler time discretization. Implicit Euler with stabilization by SUPG scheme for conservative ALE form is unconditionally stable, while second-order Crank–Nicolson time discretization gives conditionally stable estimates, see [20]. In this work, we considered higher order time discretization with dG(q) and LPS scheme, and it is shown to be unconditionally stable for any $q \geq 0$.

4.2 Error estimate for conservative ALE-LPS form and dG discretization in time

To derive the error estimate, we need the following ALE projection.

ALE projection

Let the ALE projection operator, $P : C(H_0^1; Q_T) \rightarrow S_{r,q}$ be defined as,

$$\begin{aligned}
 Pu(0, x) &= u_0(x) \text{ in } \Omega_0 \\
 Pu(t_{n+1}, x) &= u(t_{n+1}, x) \text{ in } \Omega_{t_{n+1}} \text{ for } n = 0, 1, \dots, N - 1, \\
 \int_{I_n} (Pu - u, v)_{\Omega_t} dt &= 0, \quad \forall v \in S_{r,q-1}(I_n).
 \end{aligned}
 \tag{29}$$

Since $\|u\|_t$ is allowed to be discontinuous at nodes t_n and from the definition of Pu , it can be seen that $\|Pu\|_t$ is also discontinuous at the nodes $t = t_n$.

Approximation properties

We refer proposition (3.2) in [8], for the detailed explanation of following approximation properties. Now, if $A_t \in L^\infty(I_n; W_\infty^2(\Omega_{t_{n+1}}))$ then,

$$\begin{aligned}
 \|(u - Pu)(t)\|_t^2 &\leq C_n (\Delta t)^{2j+1} \int_{I_n} \left\| \partial_t^{j+1} u(t) \Big|_Y \right\|_t^2 dt, \\
 \|\nabla(u - Pu)(t)\|_t^2 &\leq D_n (\Delta t)^{2j+1} \int_{I_n} \left(\left\| \partial_t^{j+1} u(t) \Big|_Y \right\|_t^2 + \nabla_x \left\| \partial_t^{j+1} u(t) \Big|_Y \right\|_t^2 \right) dt,
 \end{aligned}
 \tag{30}$$

for $j = 0, 1, 2, \dots, q$, with C_n, D_n depending on the ALE constants A_n and B_n given as,

$$\begin{aligned}
 C_n &\propto A_n^3 + A_n, \quad \text{and } D_n \propto (1 + M_n^2)A_n^6 + M_n^2 A_n^3 + A_n^2, \\
 \text{where } M_n &= \|\mathcal{A}_{t_n \rightarrow t}\|_{L^\infty(I_n, W_\infty^2(\Omega_{t_n}))}.
 \end{aligned}$$

We consider the bilinear form as,

$$\begin{aligned}
 B(U_h, v_h) &= \int_0^{t_N} (f, v_h) dt \\
 &= \sum_{n=0}^{N-1} \left((U_h(t_{n+1}), v_h(t_{n+1}))_{t_{n+1}} - (U_h(t_n), v_h(t_n^+))_{t_n} \right) \\
 &\quad + \int_{I_n} a_{LPS}(U_h(t), v_h)_t dt \\
 &\quad - \int_{I_n} (\nabla \cdot (\mathbf{w}_h U_h), v_h)_t dt - \int_{I_n} \left(U_h, \frac{\partial v_h}{\partial t} \Big|_Y \right)_t dt.
 \end{aligned}
 \tag{31}$$

We define the mesh-dependent strong norm as,

$$|||U_h|||_s^2 = ||U_h(t_N)||_{t_N}^2 + \int_0^{t_N} |||U_h(t)|||_t^2 dt + \sum_{n=0}^{N-1} ||(U_h(t_n^+)) - U_h(t_n)||_{t_n}^2.$$

Lemma 3 *Let the Assumptions 1 and 2 holds true and $\tau_K \sim O(h_{K,t})$, let $U_h(t)$ and $u(t)$ be the solutions of the fully discrete problem (23) and the continuous problem (8). Moreover, let $u_0 \in H^{r+1}$ and $u \in H^1(H^{r+1})$. Then, the following estimate holds true*

$$|||U_h - R_h Pu|||_s \leq C(\epsilon^{1/2} + h^{1/2})h^r (||u(t)||_{H^1(H^{r+1})}) + (\Delta t)^{q+1} ||u||_{H^{q+1}(H^1)}. \tag{32}$$

Proof Let $\xi = U_h - R_h Pu$, the bilinear form can be written as,

$$B(U_h - R_h Pu, \xi) = B(U_h - R_h u, \xi) + B(R_h u - R_h Pu, \xi),$$

bounding each term one by one, the first term is

$$\begin{aligned} B(U_h - R_h u, \xi) &= B(U_h, \xi) - B(R_h u, \xi) \\ &= \int_0^{t_N} (f, \xi) dt - \sum_{n=0}^{N-1} \left[(R_h u_{n+1}, \xi_{n+1})_{t_{n+1}} - (R_h u_n, \xi_n^+)_{t_n} \right. \\ &\quad \left. + \int_{I_n} a_{LPS}(R_h u, \xi)_t dt - \int_{I_n} (\nabla \cdot (\mathbf{w}_h R_h u), \xi)_t dt - \int_{I_n} \left(R_h u, \frac{\partial \xi}{\partial t} \Big|_Y \right)_t dt \right] \\ &= \sum_{n=0}^{N-1} \left((u(t_{n+1}) - R_h u(t_{n+1}), \xi(t_{n+1})) - (u(t_n) - R_h u(t_n), \xi(t_n^+)) \right. \\ &\quad \left. - \int_{I_n} \left(u - R_h u, \frac{\partial \xi}{\partial t} \Big|_Y \right) dt \right). \end{aligned}$$

Here first we used the definition of Ritz projection equation (14) and then Eq. (8). Further using integration by parts in time to handle the right hand side time derivative term, as we worked in (19), the above equation becomes

$$B(U_h - R_h u, \xi) = \int_0^{t_N} \left(\left(\frac{\partial}{\partial t} (u - R_h u) + (u - R_h u) \nabla \cdot \mathbf{w}_h \right), \xi \right) dt.$$

Now, using Cauchy–Schwarz and Young’s inequality and the fact that the Ritz projection error is bounded, we have

$$\begin{aligned} |B(U_h - R_h u, \xi)| &\leq \int_0^{t_N} \left(\left\| \frac{\partial}{\partial t} (u - R_h u) \right\| + \|\nabla \cdot \mathbf{w}_h\|_\infty \|u - R_h u\| \right) \|\xi(t)\| \\ &\leq C(\epsilon^{1/2} + h^{1/2})h^r (||u(t)||_{H^1(H^{r+1})}) \|\xi(t)\|. \end{aligned} \tag{33}$$

The next term can be written as

$$\begin{aligned}
 B(R_h u - R_h P u, \xi) &= \int_0^{t_N} a_{LPS}(R_h u - R_h P u, \xi) dt \\
 &\quad - \int_0^{t_N} (\nabla \cdot (\mathbf{w}_h(R_h u - R_h P u)), \xi) dt \\
 &\quad - \int_0^{t_N} \left(R_h(u - P u), \frac{\partial \xi}{\partial t} \Big|_Y \right) dt.
 \end{aligned}$$

Here, we assume that the Ritz projection commutes with the ALE projection, hence the last term vanishes due to the property of projection error. Now using the assumption that $\nabla \cdot \mathbf{w}_h$ is bounded, we have

$$\begin{aligned}
 |B(R_h u - R_h P u, \xi)| &\leq \left| \int_0^{t_N} a_{LPS}(u - P u, \xi) dt - \int_0^{t_N} (\nabla \cdot (\mathbf{w}_h(u - P u)), \xi) dt \right| \\
 &\leq C \|u - P u\| \|\xi\| \leq C \Delta t^{q+1} \|u\|_{H^{q+1}(H^1)} \|\xi\|.
 \end{aligned}$$

Thus we have

$$\| \|R_h u - R_h P u\| \|_s \leq C \Delta t^{q+1} \|u\|_{H^{q+1}(H^1)}. \tag{34}$$

Hence, by using the stability estimate and with the definition of $\| \|, \| \|_s$ -norm with Eqs. (33), (34), we obtain

$$\| \|U_h - R_h P u\| \|_s \leq C(\epsilon^{1/2} + h^{1/2}) h^r \left(\|u(t)\|_{H^1(H^{r+1})} \right) + (\Delta t)^{q+1} \|u\|_{H^{q+1}(H^1)}.$$

□

Lemma 4 *To bound the Ritz projection error, let the Assumptions 1 and 2 holds true and $\tau_K \sim O(h_{K,t})$, let $u \in H^1(H^{r+1})$ be the exact solution, then the following estimate holds*

$$\begin{aligned}
 \| \|R_h P u - R_h u\| \|_s &\leq c(\Delta t)^{q+1/2} \|u\|_{H^{q+1}(H^1)}. \\
 \| \|R_h u - u\| \|_s &\leq c(\epsilon^{1/2} + h^{1/2}) h^r \left(\|u\|_{L^2(H^{r+1})} + \|u\|_{C(H^{r+1})} \right). \tag{35}
 \end{aligned}$$

Proof Let $\eta = R_h P u - R_h u = R_h(P u - u)$, we write the bilinear form

$$\begin{aligned}
 B(\eta, \eta) &= \sum_{n=0}^{N-1} \left[\|\eta(t_{n+1})\|_{t_{n+1}}^2 - (\eta(t_n), \eta(t_n^+))_{t_n} \right. \\
 &\quad \left. + \int_{I_n} \left(\left(-\eta, \frac{\partial \eta}{\partial t} \Big|_Y \right)_t + a_{LPS}(\eta, \eta) - (\nabla \cdot (\mathbf{w}_h \eta), \eta)_t \right) dt \right].
 \end{aligned}$$

By using the stability estimate and with the definition of $||| \cdot |||_s$ -norm, the above equation becomes,

$$\begin{aligned} |||\eta|||_s^2 &\leq \sum_{n=0}^{N-1} \left(\frac{1}{2} \|\eta(t_{n+1})\|_{t_{n+1}}^2 - \frac{1}{2} \|\eta(t_n)\|_{t_n}^2 + \int_{I_n} \|\eta(t)\|^2 dt + \|\eta(t_n^+) - \eta(t_n)\|_{t_n}^2 \right) \\ &\leq \int_0^{t_N} \|\eta(t)\|^2 dt \leq \int_0^{t_N} \|R_h(Pu - u)(t)\|^2 dt \leq \int_0^{t_N} \|(Pu - u)(t)\|^2 dt \\ &\leq c(\Delta t)^{2q+1} |u|_{H^{q+1}(H^1)}^2. \end{aligned}$$

Here we have used the definition of $||| \cdot |||_s$ -norm by absorbing the right hand side terms and the property of Ritz projection (16). Thus we have,

$$|||R_h Pu - R_h u|||_s \leq c(\Delta t)^{q+1/2} |u|_{H^{q+1}(H^1)}.$$

To prove the second relation, we proceed as

$$\begin{aligned} |||R_h u - u|||_s^2 &= \|(R_h u - u)(t_N)\|_{t_N}^2 + \int_0^{t_N} \|(R_h u - u)(t)\|^2 dt \\ &\quad + \sum_{n=0}^{N-1} \|(R_h u - u)(t_n^+) - (R_h u - u)(t_n)\|_{t_n}^2. \end{aligned}$$

Since the jump in projection error vanishes, we will have

$$\begin{aligned} |||R_h u - u|||_s &\leq \left(\int_0^{t_N} \|(R_h u - u)\|^2 ds + \|(R_h u - u)(t_N)\|^2 \right)^{1/2} \\ &\leq (\epsilon^{1/2} + h^{1/2}) h^r (\|u\|_{L^2(H^{r+1})} + \|u\|_{C(H^{r+1})}). \end{aligned}$$

□

Theorem 3 (Error estimates for the ALE-LPS form and dG discretization) *Let the discrete form of (2) and the Assumptions 1 and 2 holds true. Further, assume that the stabilization parameter satisfies $\tau_K \sim O(h_{K,t})$. Then the error estimate is given by,*

$$\begin{aligned} |||U_h - u|||_s &\leq (\Delta t)^{q+1/2} |u|_{H^{q+1}(H^1)} \\ &\quad + (\epsilon^{1/2} + h^{1/2}) h^r (\|u\|_{H^1(H^{r+1})} + \|u\|_{C(H^{r+1})}). \end{aligned} \tag{36}$$

Proof The proof of the theorem can be followed by using the triangle inequality,

$$|||U_h - u|||_s = |||(U_h - R_h Pu) + (R_h Pu - R_h u) + (R_h u - u)|||_s.$$

Combining the equation from Lemmas (3) and (4) and using the triangle inequality, proof of the Theorem (3) follows. □

5 Numerical results

This section presents the numerical results to support the analysis presented in the previous sections. We consider four numerical examples to demonstrate the considered numerical scheme in time-dependent domains. In particular, we triangulate the domain with the first order finite element P_1^b projected onto P_0 with dG(1) temporal discretization for all numerical test cases.

We first consider an example with expanding and contracting domain without the convection term. Even though the convective term $\mathbf{b} = \mathbf{0}$, the ALE formulation will induce a mesh velocity type convection term. Next, we consider an example to numerically show the convergence order of the scheme. We use the time step as order h , since dG(1) is of second order in time. In the third example, we consider spatially varying convective velocity $\mathbf{b} = (y, -x)$, to see the overall effect of the convection term in time-dependent domains. In the last example, we consider a scalar problem with boundary and interior layers in a time-dependent domain. The numerical solution obtained with the standard Galerkin and the LPS method are presented.

5.1 Example 1

We consider the scalar equation (1) with $\epsilon = 0.01$, $\mathbf{b} = (0, 0)$, $c = f = 0$ with the end time $T = 2$ and $\Omega_0 := (0, 1)^2$ as the initial (reference) domain which results in,

$$\begin{aligned} \frac{\partial u}{\partial t} - 0.01 \Delta u &= 0 && \text{in } (0, T] \times \Omega_t, \\ u &= 0 && \text{on } [0, T] \times \partial\Omega_t, \\ u(0) &= 1600 Y_1(1 - Y_1) Y_2(1 - Y_2) && \text{in } \Omega_0. \end{aligned}$$

Further, the deformation of the time-dependent domain Ω_t is defined by

$$x(Y, t) = \mathcal{A}_t(Y) : \begin{cases} x_1 = Y_1(2 - \cos(20\pi t)) \\ x_2 = Y_2(2 - \cos(20\pi t)) \end{cases}.$$

In this example, the initial domain is triangulated with 8,192 cells which results in 16,641 dofs for P_1^b finite element space. The computed numerical results for different time-steps in dG(1) and in Crank–Nicolson with $\tau_0 = 0.05$ in stabilization parameter $\tau_K = \tau_0 h_K$ are shown in Fig. 1.

It can be observed that the solution becomes monotone with dG(1) time discretization. However, the solution is oscillatory in the Crank–Nicolson time discretization obtained with a large time-step since Crank–Nicolson is conditionally stable only (see [20] for detailed explanation). Here, in the case of dG time discretization, we choose the ALE map to be linear in time thus the Radau quadrature formula can integrate it exactly in time and hence there are no oscillations in the solution, which supports the stability estimate derived in Theorem 2.

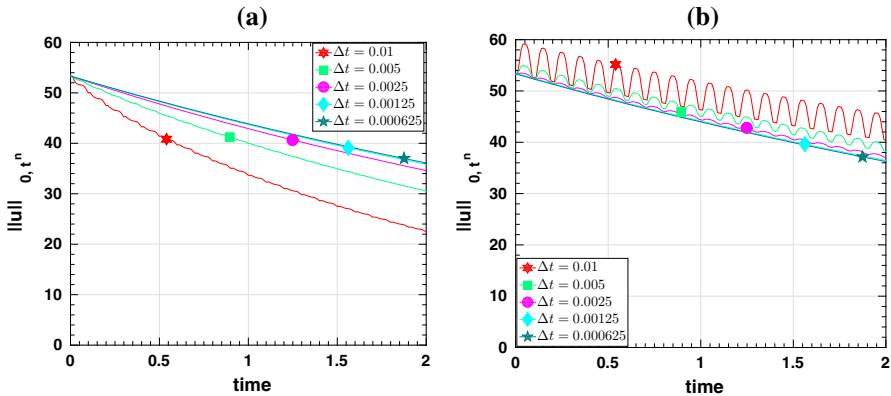


Fig. 1 L^2 -norm of the solution obtained with conservative ALE-LPS for second order time discretizations with varying time-steps: **a** discontinuous Galerkin dG(1), and **b** Crank–Nicolson

5.2 Example 2

In this example we consider the problem (1) with $\epsilon = 1$, $\mathbf{b} = (0, 0)$, $c = 0$ to show the convergence order of the LPS-DG numerical scheme. Here, we choose the time step Δt as order h_{min} . We consider the unit square $\Omega_0 := \{(0, 1) \times (0, 1)\}$ as a reference domain and the computations are performed by successive uniform refinement of the initial coarse mesh. Further, we triangulate the domain with P_1^b finite elements, and the finest level mesh results into 16, 641 dofs. The deformation of the domain is given by the ALE mapping as

$$x(Y, t) = \mathcal{A}_t(Y) : \begin{cases} x_1 = Y_1(1 + 0.5P_t) \\ x_2 = Y_2(1 + 0.5P_t) \end{cases} \quad \text{where,} \\ P_t = 1024 t^{11} - 2816 t^9 + 2816 t^7 - 1232 t^5 + 220 t^3 - 11 t,$$

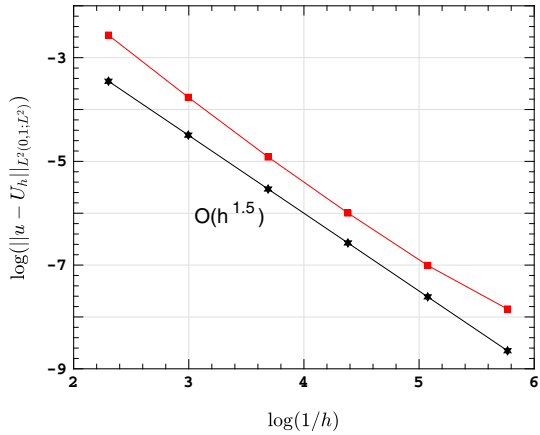
is the Chebychev polynomial of first kind. The source term is chosen in such a way that the exact solution is $u(x) = \exp(-0.01 t) \sin(\pi x) \cos(\pi y)$.

We calculated the $L^2(0, T; L^2(\Omega_t))$ norm of the error at time $T = 1$. Let q is the polynomial order of the finite element basis function in time, then the optimal order of convergence in L^2 -norm is $q + 1/2$. As it can be seen from Fig. 2 that the order of convergence is approximately 1.5 for dG(1) case, which supports the error estimate derived in Theorem 3.

Remark 4 In the first two numerical test cases, we considered the zero convection and zero reaction term to explain the effect of mesh velocity type convection and reaction terms introduced through conservative ALE scheme. The analysis condition (2) does not hold in these two examples because the estimates explode with μ (Theorem (2)). This can be fixed by updating the proof with

$$\left| \int_{I_n} (f, U_h)_t dt \right| \leq \frac{1}{2\epsilon} \int_{I_n} \|f(t)\|_{0,t}^2 dt + \frac{\epsilon}{2} \int_{I_n} \|U_h(t)\|_{0,t}^2 dt.$$

Fig. 2 The order of convergence for the considered Example 2



by using the Poincare inequality for the last term, it can be combined with left hand side |||.,.|||-norm.

5.3 Example 3

Let $\Omega_0 = (0, 1)^2$, $\epsilon = 10^{-8}$, $b(x, y) = (-y, x)^T$, $c = 0$, $\Gamma_N := \{0\} \times (0, 1)$ and $f = 0$ be in (1). On the outflow boundary, we impose the homogeneous Neumann condition. Further, we prescribe the discontinuous Dirichlet data

$$u(x, t) = \begin{cases} 1 & \text{if } (x, y) \in (1/3, 2/3) \times \{0\}, \\ 0 & \text{else} \end{cases}$$

on Γ_D . This discontinuous Dirichlet data is transported counter-clockwise to the homogeneous Neumann outflow boundary. Further, the deformation of the time-dependent domain Ω_t is given by

$$x(Y, t) = \mathcal{A}_t(Y) : \begin{cases} x_1 = Y_1(1.125 - 0.125 \cos(5\pi t)) \\ x_2 = Y_2(1.125 - 0.125 \cos(5\pi t)) \end{cases}$$

Note that the convective velocity is spatially varying and in addition, interior layers are present in this example. The computed solutions with LPS and dG(1) at different instance, $t = 1.06, 2.05, 2.5$ are given in Fig. 3. Since the domain expands and shrinks with fixed inflow concentration, the concentration is transported in a staggered manner. Nevertheless, spurious oscillations are suppressed in the stabilized solution, see Fig. 4.

5.4 Example 4

In this example, a typical fluid-structure interaction problem that is a flow passing through a cylinder, which moves with time, is studied. The mesh movement in ALE mapping is handled using the linear elastic technique [21]. Define a time-dependent two-dimensional channel

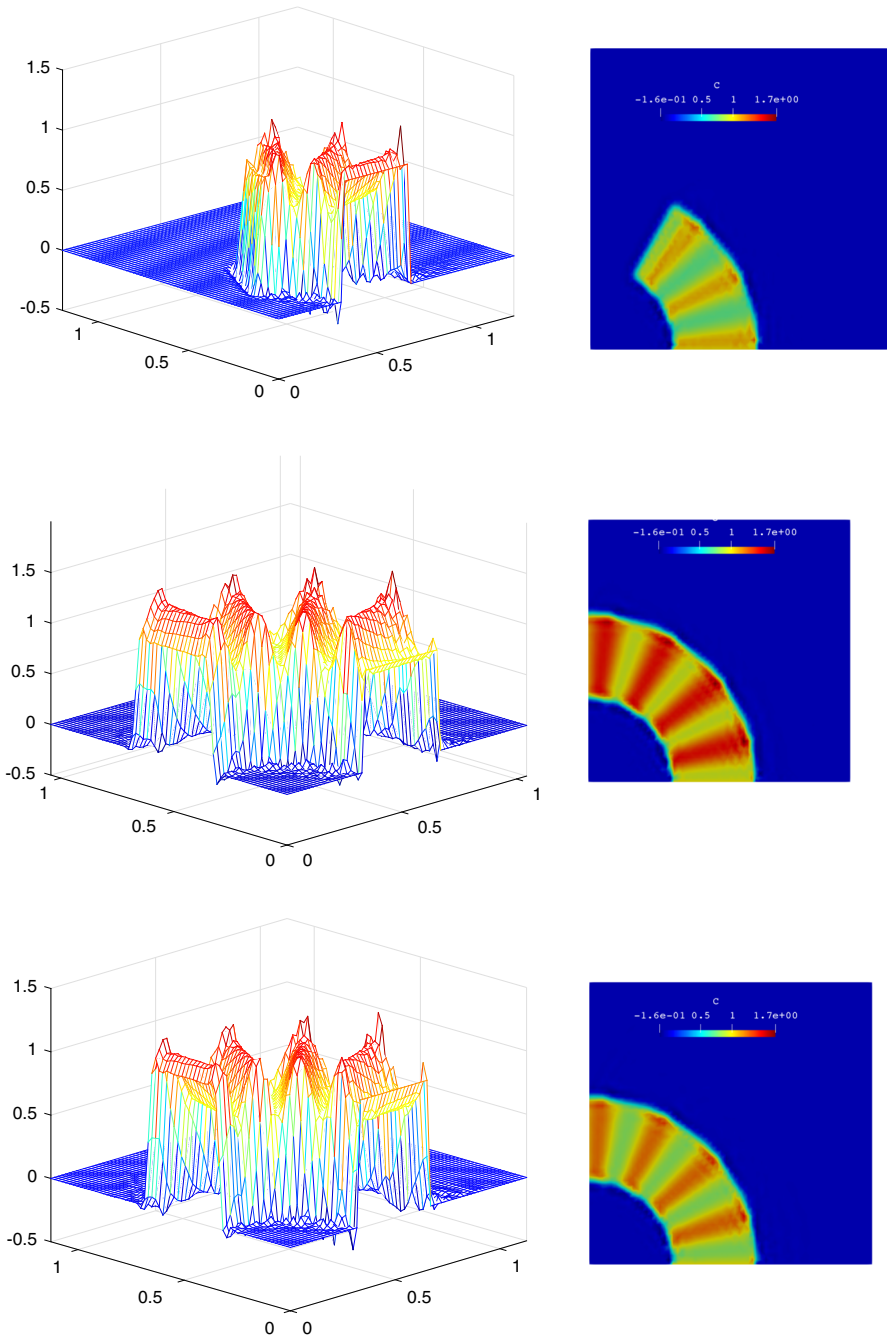
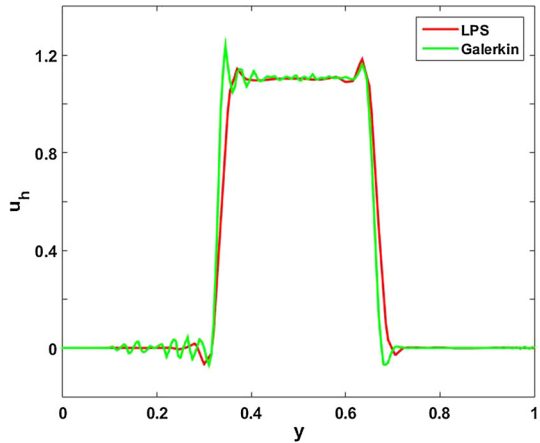


Fig. 3 Solution of Example 3 with P_1^b projected onto P_0 . The stabilization parameter value $\tau_0 = 0.0045$ at different instances $t = 1.06, 2.05, 2.5$

Fig. 4 Solution of the Example 3 at the outflow boundary with P_1^b projected onto P_0 . The stabilization parameter value is $\tau_0 = 0.0045$



$$\Omega_t := \{(-3, 9) \times (-3, 3)\} \setminus \bar{\Omega}_t^S$$

that excludes a periodically oscillating (up and down) circular disc Ω_t^S , where the position of the disc, $x(Y, t) \in \Omega_t^S$, and the reference disc Ω_0^S are given by

$$x(Y, t) = \mathcal{A}_t(Y) : \begin{cases} x_1 = Y_1 \\ x_2 = Y_2 + 0.5 \sin(2\pi t/5), \end{cases}$$

$$\Omega_0^S := \{(Y_1, Y_2) \in \mathbb{R}^2; Y_1^2 + Y_2^2 \leq 1\}.$$

Define $\Gamma_D := \{-3\} \times (-3, 3)$ as the inflow boundary and the remaining part $\Gamma_N := \partial\Omega_t \setminus \Gamma_D$ as the Neumann boundary. We now solve the transient scalar equation (1) with $\epsilon = 10^{-8}$, $\mathbf{b} = (1, 0)^T$ and $c = 0$.

We impose zero initial value, the homogeneous Neumann condition on Γ_N , and

$$u_D(x_1, x_2) = \begin{cases} 1 & \text{on } \partial\Omega_t^S, \\ 0 & \text{on } \Gamma_D. \end{cases}$$

A predefined adaptive mesh with a high resolution near the oscillating cylinder is considered. Nevertheless, the mesh is comparatively coarser away from the cylinder. The considered domain with refined grids in which simulations are performed is shown in Fig. 5. For the considered data, there will be a boundary layer on the upstream of the oscillating circular disc and two interior layers on the downstream of the disc. Since the solid disc oscillates periodically, the position of the boundary and interior layers also changes with time.

It can be seen from Fig. 6 that the standard Galerkin solution contains very high undershoots/overshoots (approximately 14.9% and 12.4%) in the numerical solution. Further the solution obtained with ALE-LPS at different time instances are given, see Fig. 7. It can be seen from Fig. 7 that the undershoots/overshoots are suppressed

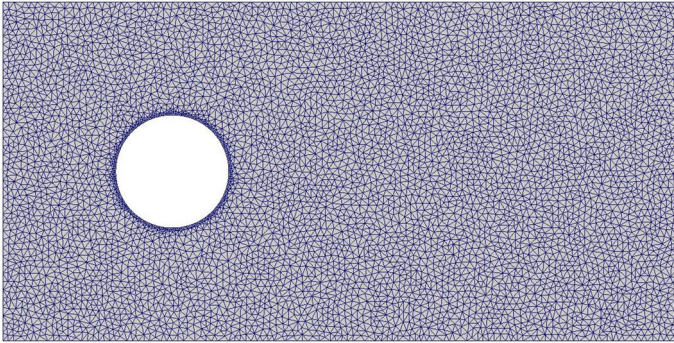


Fig. 5 The refined mesh for the simulations of Example 4

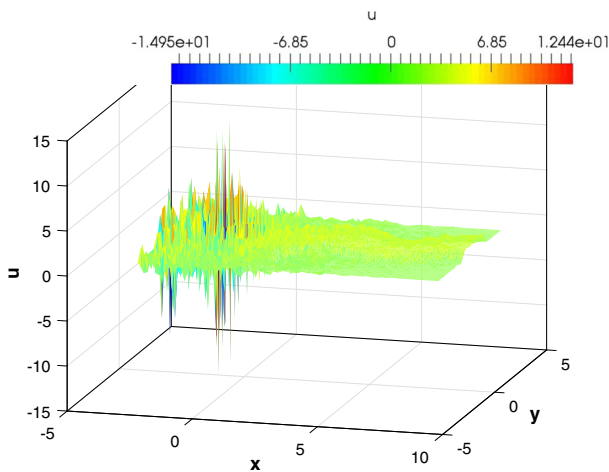


Fig. 6 Standard Galerkin solution for the Example 4 at $t = 10$ with dG(1) time discretization

almost (around 0.24%), which shows the stabilization effect of the local projection method in time-dependent domains.

6 Summary

A stabilized finite element scheme based on Local Projection Stabilization (LPS) with higher order discontinuous Galerkin (dG) discretization in time is analyzed for the solution of convection–diffusion–reaction problems in time-dependent domains. One-level LPS, which involves enriched approximation space and discontinuous projection space is used. The domain movement is handled with ALE formulations. The stability and convergence estimates are shown. An optimal order error estimate with conservative ALE formulation and dG in time-dependent domains is derived.

The proposed numerical scheme is validated using four test cases. In the first example, a unit square which expands and contracts periodically is considered, to see

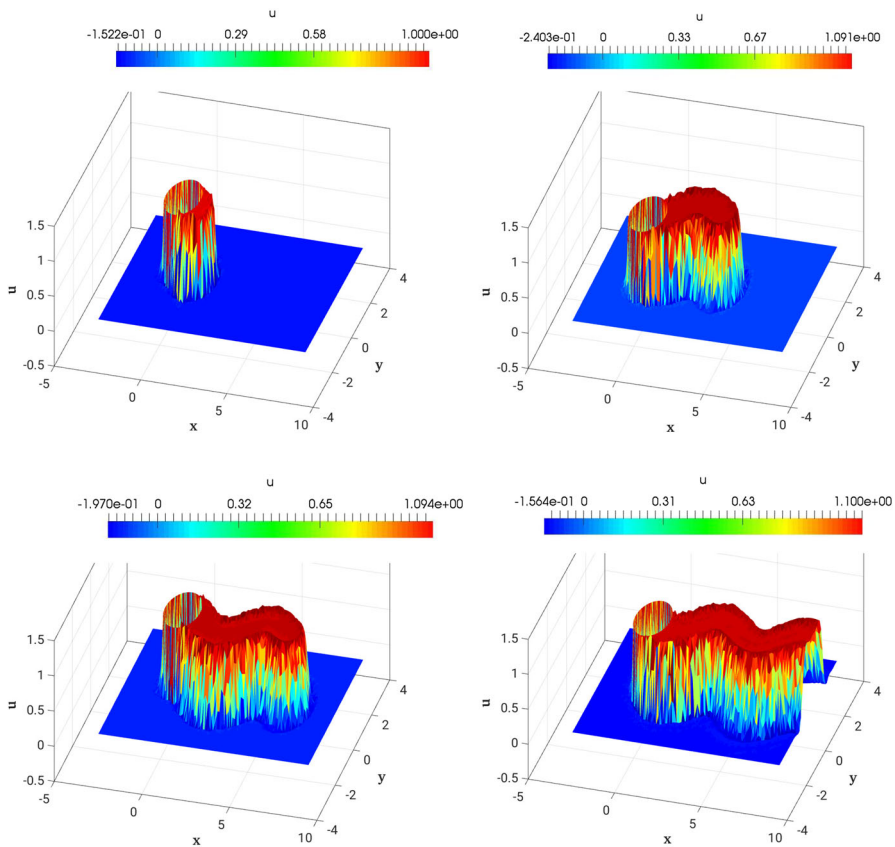


Fig. 7 A sequence of ALE-LPS solution of Example 4 obtained with $\delta_0 = 0.1$ and dG time discretization at different instances $t = 0.1, 4, 6.3, 10$

the effect of ALE mapping and unconditional stable estimates with LPS and dG(1) discretization. In the next example, we observe the order of convergence with LPS and dG(1) discretization which confirms the theoretical estimates. Further, a spatial-dependent convective velocity with interior layers in an expanding and shrinking domain is considered. The fourth test case shows that the local projection stabilization scheme with dG in time works very well for convection dominated problems.

References

1. Ahmed, N., Matthies, G., Tobiska, L., Xie, H.: Discontinuous Galerkin time stepping with local projection stabilization for transient convection–diffusion–reaction problems. *Comput. Methods Appl. Mech. Eng.* **200**, 1747–1756 (2011)
2. Badia, S., Codina, R.: Analysis of a stabilized finite element approximation of the of the transient convection–diffusion equation using an ALE framework. *SIAM J. Numer. Anal.* **44**(5), 2159–2197 (2006)

3. Becker, R., Braack, M.: A finite element pressure gradient stabilization for the Stokes equations based on local projections. *Calcolo* **38**, 173–199 (2001)
4. Becker, R., Braack, M.: A two-level stabilization scheme for the Navier–Stokes equations. In: Feistauer, M., Dolejší, V., Knobloch, P., Najzar, K. (eds.) *Numerical Mathematics and Advanced Applications*, pp. 123–130. Springer, Berlin (2004)
5. Becker, R., Vexler, B.: Optimal control of the convection–diffusion equation using stabilized finite element methods. *Numer. Math.* **106**(3), 349–367 (2007)
6. Boffi, D., Gastaldi, L.: Stability and geometric conservation laws for ALE formulations. *Comput. Methods Appl. Mech. Eng.* **193**, 4717–4739 (2004)
7. Bonito, A., Kyza, I., Nochetto, R.: Time-discrete higher order ale formulations: stability. *SIAM J. Numer. Anal.* **51**, 577–604 (2013)
8. Bonito, A., Kyza, I., Nochetto, R.: Time-discrete higher order ale formulations: a priori error analysis. *Numer. Math.* **125**, 225–257 (2013)
9. Braack, M.: Optimal control in fluid mechanics by finite elements with symmetric stabilization. *SIAM J. Control Optim.* **48**(2), 672–687 (2009)
10. Braack, M., Lube, G.: Finite elements with local projection stabilization for incompressible flow problems. *J. Comput. Math.* **27**(2–3), 116–147 (2009)
11. Brooks, A.N., Hughes, T.J.R.: Streamline upwind/Petrov–Galerkin formulations for convection dominated flows with particular emphasis on the incompressible Navier–Stokes equations. *Comput. Methods Appl. Mech. Eng.* **32**, 199–259 (1982)
12. Burman, E.: Consistent SUPG-method for transient transport problems: stability and convergence. *Comput. Methods Appl. Mech. Eng.* **199**, 1114–1123 (2010)
13. Burman, E., Ern, A.: Continuous interior penalty hp-finite element methods for advection and advection–diffusion equations. *Math. Comput.* **76**, 1119–1140 (2007)
14. Burman, E., Fernandez, M., Hansbo, P.: Continuous interior penalty finite element method for Oseen’s equations. *SIAM J. Numer. Anal.* **44**, 1248–1274 (2006)
15. Burman, E., Hansbo, P.: Edge stabilization for Galerkin approximations of convection–diffusion–reaction problems. *Comput. Methods Appl. Mech. Eng.* **193**, 1437–1453 (2004)
16. Codina, R.: Stabilization of incompressibility and convection through orthogonal sub-scales in finite element methods. *Comput. Methods Appl. Mech. Eng.* **190**, 1579–1599 (2000)
17. Codina, R., Blasco, J.: Analysis of a stabilized finite element approximation of the transient convection–diffusion–reaction equation using orthogonal subscales. *Comput. Vis. Sci.* **4**(3), 167–174 (2002)
18. Formaggia, L., Nobile, F.: A stability analysis for the arbitrary Lagrangian Eulerian formulation with finite elements. *East-West J. Numer. Math.* **7**(2), 105–131 (1999)
19. Formaggia, L., Nobile, F.: Stability analysis of second-order time accurate schemes for ALE-FEM. *Comput. Methods Appl. Mech. Eng.* **193**, 4097–4116 (2004)
20. Ganesan, S., Srivastava, S.: ALE-SUPG finite element method for convection–diffusion problems in time-dependent domains: conservative form. *Appl. Math. Comput.* **303**, 128–145 (2017)
21. Ganesan, S., Tobiska, L.: Stabilization by local projection for convection–diffusion and incompressible flow problems. *J. Sci. Comput.* **43**(3), 326–342 (2010)
22. Gastaldi, L.: A priori error estimates for the arbitrary Lagrangian Eulerian formulation with finite elements. *East-West J. Numer. Math.* **9**, 123–156 (2001)
23. Guermond, J.L.: Stabilization of Galerkin approximations of transport equations by subgrid modeling. *M2AN Math. Model. Numer. Anal.* **33**(6), 1293–1316 (1999)
24. Hughes, T.J.R., Franca, L.P., Hulbert, G.M.: A new finite element formulation for computational fluid dynamics: VIII. The Galerkin/least-squares method for advective–diffusion equations. *Comput. Methods Appl. Mech. Eng.* **73**, 173–189 (1989)
25. John, V., Novo, J.: Error analysis of the SUPG finite element discretization of evolutionary convection–diffusion–reaction equations. *SIAM J. Numer. Anal.* **49**(3), 1149–1176 (2011)
26. Knobloch, P.: A generalization of the local projection stabilization for convection–diffusion–reaction equations. *SIAM J. Numer. Anal.* **48**(2), 659–680 (2010)
27. Matthies, G., Skrzypacz, P., Tobiska, L.: A unified convergence analysis for local projection stabilisations applied to the Oseen problem. *Math. Model. Numer. Anal.* **41**, 713–742 (2007)
28. Roos, H.G., Stynes, M., Tobiska, L.: *Numerical Methods for Singularly Perturbed Differential Equations*. Springer, Berlin (2008)
29. Srivastava, S., Ganesan, S.: On the temporal discretizations of convection dominated convection–diffusion equations in time-dependent domain. *Pro-Mathematica* **30**(59), 99–137 (2018)

30. Thomee, V.: Galerkin Finite Element Methods for Parabolic Problems, 3rd edn. Springer, Berlin (2008)
31. Tobiska, L., Verfürth, R.: Analysis of a streamline diffusion finite element method for the Stokes and Navier–stokes equations. *SIAM J. Numer. Anal.* **33**, 407–421 (1996)

Publisher's Note Springer Nature remains neutral with regard to jurisdictional claims in published maps and institutional affiliations.